The Journal of Neuroscience, September 1, 1999, *19*(17):7334–7341

High Conductance Sustained Single-Channel Activity Responsible for the Low-Threshold Persistent Na^+ Current in Entorhinal Cortex Neurons

Jacopo Magistretti,[1,2] **David S. Ragsdale,**[1] **and Angel Alonso**[1]

[1]*Department of Neurology and Neurosurgery, Montreal Neurological Institute, McGill University, H3A 2B4, Montreal, Quebec, Canada, and* [2]*Laboratorio di Biofisica e Neurofisiologia dei Sistemi Corticali, Dipartimento di Neurofisiologia Sperimentale, Istituto Nazionale Neurologico "Carlo Besta", 20133 Milano, Italy*

Stellate cells from entorhinal cortex (EC) layer II express both a transient Na^+ current (I_{Na}) and a low-threshold persistent Na^+ current (I_{NaP}) that helps to generate intrinsic theta-like oscillatory activity. We have used single-channel patch-clamp recording to investigate the Na^+ channels responsible for I_{NaP} in EC stellate cells. Macropatch (more than six channels) recordings showed high levels of transient Na^+ channel activity, consisting of brief openings near the beginning of depolarizing pulses, and lower levels of persistent Na^+ channel activity, characterized by prolonged openings throughout 500 msec long depolarizations. The persistent activity contributed a noninactivating component to averaged macropatch recordings that was comparable with whole-cell I_{NaP} in both voltage dependence of activation (10 mV negative to the transient current) and amplitude (1% of the transient current at −20 mV). In 14 oligochannel (less than six channels) patches, the ratio of transient to persistent channel activity varied from patch to patch, with 10 patches exhibiting exclusively transient openings and one patch showing exclusively persistent openings. In two patches containing only a single persistent channel, prolonged openings were observed in >50% of test depolarizations. Moreover, persistent openings had a significantly higher single-channel conductance (19.7 pS) than transient openings (15.6 pS). We conclude that this stable high-conductance persistent channel activity is responsible for I_{NaP} in EC stellate cells. This persistent channel behavior is more enduring and has a higher conductance than the infrequent and short-lived transitions to persistent gating modes that have been described previously in brain neurons.

Key words: Na^+ channel; persistent Na^+ current; patch clamp; single-channel recording; rat; entorhinal cortex; stellate cells; temporal lobe

The familiar role for voltage-gated Na^+ channels is in the generation of the transient Na^+ current (I_{Na}) responsible for the initiation and propagation of action potentials. However, many mammalian brain neurons also exhibit a low-voltage-activated, slowly inactivating "persistent" Na^+ current (I_{NaP}), that contributes to oscillatory activity (Alonso and Llinás, 1989; Silva et al., 1991), boosting of synaptic potentials (Stuart and Sakmann, 1995), and firing-pattern shaping (Llinás and Sugimori, 1980; Klink and Alonso, 1993; Franceschetti et al., 1995; Parri and Crunelli, 1998; for review, see Crill, 1996). I_{NaP} has also been linked to the pathophysiology of epilepsy (Segal, 1994) and other neurological diseases (Stys et al., 1993). Thus, it may be an important target for the development of new pharmacological agents (Taylor, 1993).

Despite its critical role in brain function, the biophysical and molecular bases of I_{NaP} have remained elusive. One widely held hypothesis is that I_{NaP} is caused by rare, short-lived transitions of conventional transient Na^+ channels to a slowly inactivating gating mode (Alzheimer et al., 1993; Segal and Douglas, 1997). In multichannel patches from sensorimotor cortex neurons, this slow-mode gating was characterized by sustained bursts of channel activity in ~1% of depolarizing test pulses (Alzheimer et al., 1993). In contrast, other single-channel studies in brain neurons (Masukawa et al., 1991; Sugimori et al., 1994) have suggested the presence of a more stable persistent channel activity. However, these studies did not give a detailed analysis of this single-channel behavior. Furthermore, an important element missing from previous studies has been direct evidence that persistent single-channel openings recorded in patches sum to give the low-threshold persistent Na^+ currents observed in whole-cell recordings.

A key population of neurons in the temporal lobe, the stellate cells of entorhinal cortex (EC) layer II, possess a robust I_{NaP} (Alonso and Llinás, 1989; Klink and Alonso, 1993; Magistretti and Alonso, 1999). This persistent Na^+ current generates intrinsic pacemaker activity that is thought to contribute to the genesis of the limbic theta rhythm (Bland, 1986; Alonso and García-Austt, 1987; Alonso and Llinás, 1989), a brain rhythm that has been implicated in memory function (Winson, 1978; Holscher et al., 1997). The oscillatory properties of EC stellate cells may also play a role in temporal lobe epileptogenesis (Dickson and Alonso, 1997; Klink and Alonso, 1997). In this study, we investigated the Na^+ channels responsible for I_{NaP} in EC stellate cells using single-channel patch-clamp electrophysiological recording. In cell-attached patches, we identified Na^+ channel activity that was characterized by repeated prolonged openings throughout 500-msec-long sweeps. In patches showing persistent activity, pro-

Received April 14, 1999; revised June 17, 1999; accepted June 18, 1999.

This work was supported by grants from the Medical Research Council of Canada (MRC) and the Human Frontier Science Program Organization (HFSPO) to A.A. and grants from the MRC and the Natural Science and Engineering Research Council of Canada to D.R. J.M. thanks Dr. M. de Curtis, the Instituto Nazionale Neurologico "C. Besta", and the HFSPO for support.

Correspondence should be addressed Dr. David S. Ragsdale, Department of Neurology and Neurosurgery, Montreal Neurological Institute, McGill University, 3801 University Street, Montreal, Quebec, H3A 2B4, Canada.

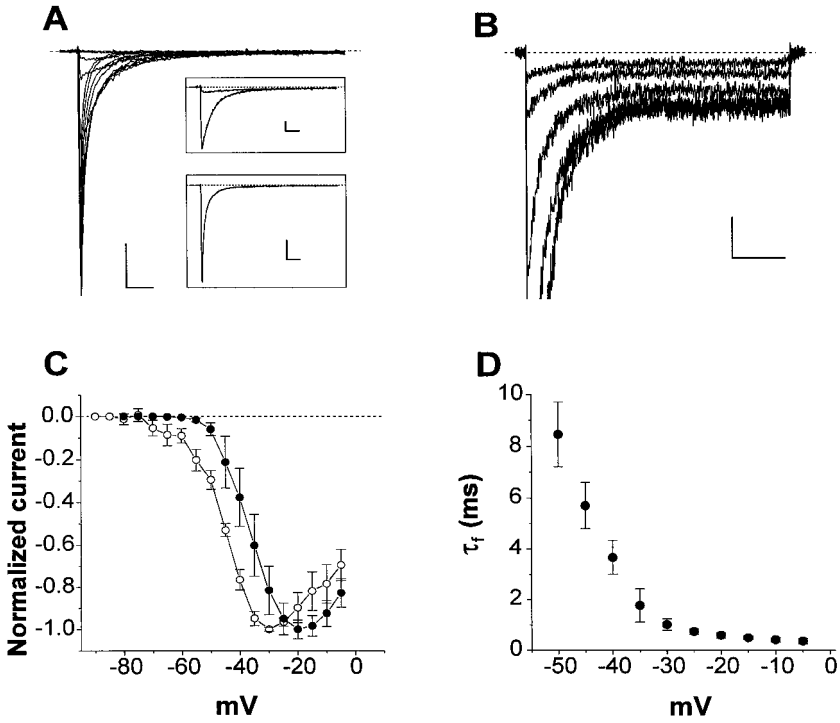

Figure 1. Whole-cell I_{Na} and I_{NaP} in EC layer II principal neurons. *A*, Whole-cell Na^+ currents elicited in a representative neuron by depolarizing steps to potentials ranging from −60 to −5 mV, in 5 mV increments. The holding potential was −80 mV. Calibration: 300 pA, 5 msec. The *insets* show current traces at the test potentials of −50, −40 (*top inset*), and −20 (*bottom inset*) mV, along with biexponential fits (*superimposed lines*) of current decay. Time constants for the fast and slow components of current decay were as follows: −50 mV, τ_f = 8.51 msec, τ_s = 20.12 msec; −40 mV, τ_f = 3.5 msec, τ_s = 14.34 msec; −20 mV, τ_f = 0.69 msec, τ_s = 3.61 msec. Calibration: *top inset*, 100 pA, 5 msec; *bottom inset*, 300 pA, 5 msec. *B*, I_{NaP} recorded, at higher gain, in a different neuron. Depolarizing pulses were from −50 to −25 mV in 5 mV steps, from a holding potential of −80 mV. Calibration: 25 pA, 50 msec. *C*, Mean current–voltage relationships for I_{Na} (●; n = 8) and I_{NaP} (○; n = 5). I_{Na} amplitudes were measured at the current peak. I_{NaP} amplitudes were derived by averaging the data points between 400 and 500 msec from the start of each test pulse. In this and subsequent figures, symbols and error bars show means ± SD. *D*, Mean values for the fast inactivation time constant (τ_f) for I_{Na} (n = 7), plotted as a function of test potential.

longed openings were observed in >50% of test depolarizations. Furthermore, persistent channel activity displayed a higher single-channel conductance than transient Na^+ channel activity in the same neurons. Ensemble averages of persistent activity gave a persistent Na^+ current with an amplitude and voltage dependence similar to whole-cell I_{NaP}. We conclude that this stable high-conductance persistent channel activity is responsible for I_{NaP} in stellate cells of entorhinal cortex.

MATERIALS AND METHODS

Preparation of acutely dissociated neurons. The procedure for acute isolation of EC layer II neurons was as described previously (Magistretti and de Curtis, 1998). Briefly, male Long–Evans rats [postnatal day 25 (P25) to P35] were decapitated, and the brains were quickly removed, submerged into ice-cold dissociation buffer [in mM: 115 NaCl, 3 KCl, 3 $MgCl_2$, 0.2 $CaCl_2$, 25 glucose, and 20 PIPES, pH 7.0, bubbled with O_2], and 400-μm-thick coronal slices were cut with a vibratome. Using a fine scalpel, pieces of entorhinal cortex layer II were dissected and transferred to dissociation buffer at 32°C. Protease type XIV (1 mg/ml; Sigma–Aldrich, Oakville, Ontario, Canada) was added, and the pieces of brain tissue were incubated for 15 min with gentle agitation. The tissue was washed with dissociation buffer, left at room temperature for 1 hr, and then dissociated by trituration through Pasteur pipettes with fire-polished tips of progressively smaller inner diameter. Suspensions of dissociated cells were transferred to a recording chamber for electrophysiological experiments.

Electrophysiological recordings. Na^+ currents were recorded from acutely dissociated neurons using the patch-clamp recording technique (Hamill et al., 1981) in the whole-cell and cell-attached configurations. In whole-cell experiments, cells were perfused with a solution containing (in mM): 100 NaCl, 40 TEA-Cl, 10 HEPES, 2 $CaCl_2$, 3 $MgCl_2$, 0.2 $CdCl_2$, 5 4-aminopyridine (4-AP), and 25 glucose, pH 7.4. The pipette solution contained (in mM): 110 CsF, 10 HEPES, 11 EGTA, and 2 $MgCl_2$, pH 7.25. Whole-cell patch pipettes had a resistance of 2–4 MΩ when filled with this solution. Recordings were performed with an Axopatch 1D amplifier and pCLAMP software (Axon Instruments, Foster City, CA). Series resistance (6.5–14.0 MΩ) was compensated by ~80%. All experiments were performed at room temperature (23 ± 1°C). Persistent Na^+ currents were isolated by off-line subtraction of current traces recorded after application of 1 μM TTX.

In single-channel experiments, cells were initially perfused with a solution containing (in mM): 140 NaCl, 5 KCl, 10 HEPES, 2 $CaCl_2$, 2 $MgCl_2$, and 25 glucose, pH 7.4. The pipette solution contained (in mM): 130 NaCl, 35 TEA-Cl, 10 HEPES, 2 $CaCl_2$, 2 $MgCl_2$, and 5 4-AP, pH 7.4. Single-channel patch pipettes had resistances ranging from 10 to 35 MΩ when filled with this solution. After obtaining the cell-attached configuration, the extracellular perfusion was switched to a high-potassium solution containing (in mM): 140 K-acetate, 5 NaCl, 10 HEPES, 4 $MgCl_2$, 0.2 $CdCl_2$, and 25 glucose, pH 7.4, to hold the neuron resting membrane potential at near 0 mV. Recordings were performed at room temperature with an Axopatch 200B amplifier (Axon Instruments). Capacitive transients were minimized with the built-in compensation circuitry of the amplifier. Holding potential was −100 or −120 mV. Depolarizing voltage steps were delivered at 5 sec intervals. Current signals were low-pass filtered at 5 or 2 kHz and digitized at 100 or 10 kHz when acquiring 50 or 500 msec sweeps, respectively. For single-channel analysis, residual capacitive transients and leak currents were nullified by off-line subtraction of fits of averaged blank traces. Persistent single-channel open probability (P_o) was estimated, in both single sweeps and ensemble average traces, according to

$$P_o = I_{avg}/(N \cdot i)$$

where I_{avg} is the average current level over the last 455 msec of 500 msec test pulses, N is the number of persistent channels in the patch estimated from the maximum number of superimposed openings, and i is the single-channel current amplitude.

Mean values in the text are presented ±SD. Statistical significance of differences between groups were assessed with Student's t test. All chemicals were obtained from Sigma–Aldrich.

RESULTS

Whole-cell Na^+ currents in EC stellate cells show transient and persistent components

Figure 1 illustrates the properties of whole-cell Na^+ currents in EC stellate cells. In whole-cell recordings, the predominant Na^+ current evoked by membrane depolarization was a transient current (I_{Na}), which rose rapidly to a peak and then decayed to near baseline within a few milliseconds (Fig. 1*A*). The current–voltage (*I–V*) relationship of I_{Na} showed a threshold at approximately −50 mV and a peak at approximately −20 mV (Fig. 1*C*, ●). The

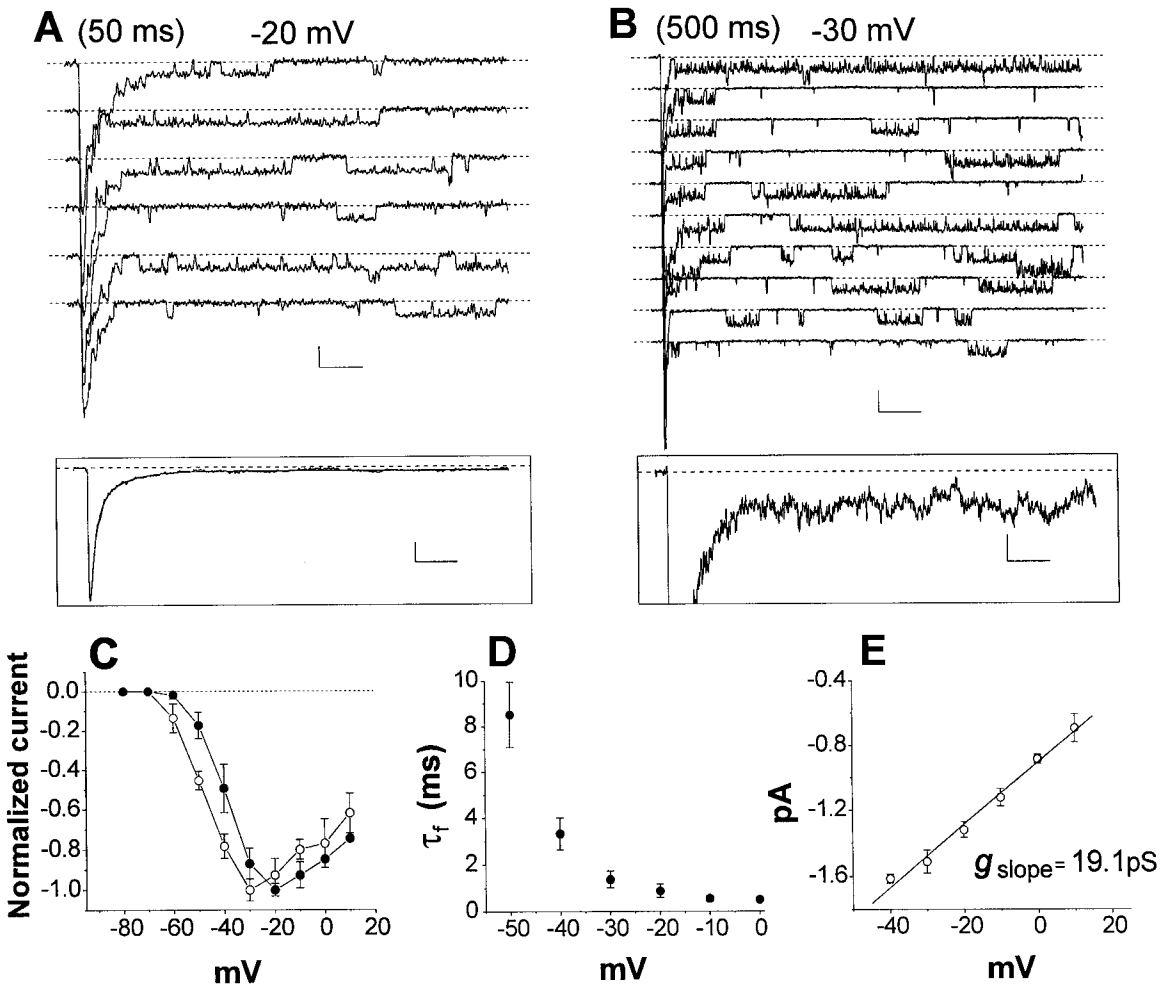

Figure 2. Na^+ channel activity in macropatch recordings. *A*, Na^+ channel currents evoked by consecutive 50 msec depolarizing pulses to −20 mV. Calibration: 2 pA, 5 msec. The *inset* shows an ensemble current trace obtained from the averaging a set of 20 consecutive traces. The decaying phase of the ensemble current is fit with a biexponential function with time constants τ_f = 0.71 msec and τ_s = 3.29 msec. Calibration: *inset*, 2 pA, 5 msec. *B*, Consecutive traces in the same patch as in *A*, elicited by 500 msec depolarizing pulses to −30 mV. Calibration: 2 pA, 50 msec. The *inset* shows the average of a set of 20 consecutive traces, displayed at a high amplification, to illustrate the persistent component of the ensemble current. Calibration: *inset*, 0.2 pA, 50 msec. *C*, Mean current–voltage relationships for the transient (●; n = 7) and persistent (○; n = 7) components of ensemble currents. *D*, Mean τ_f for ensemble transient currents, plotted as a function of test potential. *E*, Voltage dependence of persistent single-channel current amplitude. Only openings occurring at least 20 msec after the start of the test pulse were considered. Data points are from eight patches. In this and subsequent single-channel *I–V* plots, the *straight line* is a linear least squares fit of the mean data points, with the slope conductance value given in the graph, whereas conductance values reported in Results are means of slope conductances determined for each individual experiment.

decay phase of the current was best fit by the sum of two exponential functions (typical fits are shown in Fig. 1*A*, *insets*), with a prominent fast component that was strongly voltage-dependent over test potentials ranging from −50 to −5 mV (Fig. 1*D*). In addition to this transient Na^+ current, depolarizing voltage steps also elicited a long-lasting, or persistent, Na^+ current (I_{NaP}) (Fig. 1*B*). The *I–V* relationship for I_{NaP} was shifted ~10 mV negative compared with I_{Na} (Fig. 1*C*, ○), similar to previously described persistent Na^+ currents in brain neurons (French et al., 1990). Also in agreement with previous findings, the amplitude of I_{NaP} at −20 mV was 0.94 ± 0.82% of the peak current (n = 8). One micromolar TTX abolished both I_{Na} and I_{NaP}, indicating that both currents were mediated by TTX-sensitive voltage-gated Na^+ channels. A TTX-sensitive I_{NaP} of approximately the same relative amplitude and with the same biophysical characteristics was also recorded in EC layer II neurons *in situ* (data not shown; but see Magistretti and Alonso, 1999).

Macropatches exhibit both transient and persistent Na^+ channel activity

To determine the properties of the channels responsible for whole-cell I_{Na} and I_{NaP}, we examined Na^+ channel behavior in patch-clamp experiments in stellate cell somata, using the cell-attached recording configuration. Na^+ channel activity was recorded in 67 of 68 patches. Most patches (n = 52) contained more than six channels, as judged by the maximal number of superimposed channel openings. Figure 2 shows an example of Na^+ channel activity in one of these "macropatch" experiments in response to 50 (Fig. 2*A*) or 500 (Fig. 2*B*) msec depolarizing test pulses. A depolarizing step elicited a large transient inward current in the first few milliseconds after the start of the test pulse because of the superimposed opening of rapidly activating and inactivating transient Na^+ channels (Fig. 2*A*). When many consecutive traces were averaged (Fig. 2*A*, *inset*), the transient chan-

nel activity produced a transient ensemble current that closely resembled I_{Na} recorded in whole-cell experiments, in terms of both time course (Fig. 2*A*, *inset*, *D*) and *I–V* relationship (Fig. 2*C*, ●).

In addition to the transient channel activity, test pulses in macropatch experiments also elicited a lower level of sustained channel activity, characterized by repeated episodes of prolonged openings throughout even long-lasting depolarizations (Fig. 2*B*). These "persistent" channel openings were observed in most sweeps in 16 of 20 macropatches in which we were able to determine channel behavior using an extended series of 500-msec-long test pulses. Ensemble averages of the late openings produced a measurable persistent current (Fig. 2*A*,*B*, *insets*) that closely resembled whole-cell I_{NaP} in terms of both voltage-dependence of activation and relative amplitude. The mean *I–V* relationship for ensemble persistent currents (Fig. 2*C*, ○) was similar to that determined from whole-cell recordings of I_{NaP}, and, like I_{NaP} versus I_{Na}, was shifted by ~10 mV in the negative direction with respect to the mean *I–V* relationship of ensemble transient currents (Fig. 2*C*, ●). In addition, the mean amplitude of the persistent component in ensemble current traces at −20 mV was 0.90 ± 0.71% ($n = 20$) of the peak amplitude of the transient component, a percentage very similar to that of I_{NaP} versus I_{Na} in whole-cell recordings. In 10 of 10 experiments, both transient and persistent single-channel currents were absent when 1 μM TTX was included in the patch pipette (data not shown), indicating that both types of channel behavior were caused by TTX-sensitive Na^+ channels. Together, these data indicate that the noninactivating channel activity recorded in macropatches was responsible for whole-cell I_{NaP}. The single-channel conductance determined for late channel openings in eight macropatches was 19.3 ± 2.3 pS (Fig. 2*E*).

Single Na^+ channels exhibit distinct transient and persistent gating behaviors

A more limited number of patches ($n = 14$) contained from two to five channels. Ten of these "oligochannel" patches exhibited exclusively transient channel activity. The voltage- and time-dependent behavior of these transient single-channel currents was similar to the typical transient Na^+ channels that have been described previously in neurons (Fig. 3*A*) (Aldrich et al., 1983; Kirsch and Brown, 1989; Alzheimer et al., 1993; Magee and Johnston, 1995). Ensemble currents decayed according to single exponential functions, with time constants similar to the fast time constants determined for both average transient currents of macropatches and whole-cell I_{Na} (Fig. 3*A*, *insets*, *C*). In transient channel patches, late channel activity was rarely observed and was almost entirely limited to brief, infrequent reopenings (Fig. 3*A*,*B*). Furthermore, ensemble currents did not show any detectable persistent component (Fig. 3*A*, *insets*), consistent with the idea that these rare reopenings were not responsible for I_{NaP} in EC neurons. The mean slope conductance of fast channel activity was 15.6 ± 1.7 pS (Fig. 3*D*). This conductance is similar to the values reported previously for transient Na^+ channels in various CNS neuron types (Kirsch and Brown, 1989; Alzheimer et al., 1993; Magee and Johnston, 1995) but statistically significantly different ($p < 0.005$) from the conductance of late channel openings in multichannel patches.

Four oligochannel patches showed persistent Na^+ channel activity. For example, Figure 4*A* shows consecutive sweeps from a patch that contained five channels (based on the maximum number of superimposed openings) and showed a high level of persistent behavior. Persistent single-channel activity was observed in this patch at test potentials as negative as −60 mV at which it appeared as intensely flickering and incompletely resolved openings (Fig. 4*A*, *left traces*). With stronger depolarizations, channels exhibited repeated prolonged openings that sometimes lasted for the entire duration of 500-msec-long test pulses (Fig. 4*A*, *right traces*). When traces from this experiment were averaged (Fig. 4*A*, *insets*), the ensemble currents showed a rapid activation time course, followed by a very slow rate of inactivation, with a prominent persistent component at the end of the 500-msec-long test pulse. The absence of any detectable transient component in the ensemble traces (Fig. 4*A*, *inset*) argues that there was little or no transient activity in this patch. A transient component to the ensemble currents would be expected if most sweeps were a mixture of transient and persistent single-channel currents (Fig. 5*A*). The high level of persistent gating behavior throughout this experiment is also illustrated in Figure 4*B*, which shows the estimated single-channel open probability, P_o (determined as described in Materials and Methods), plotted for consecutive 500-msec-long sweeps, over a range of test potentials. P_o values were high for every sweep, indicating that a high level of persistent channel activity was present throughout the entire 17-min-long experiment. Together, these results indicate that Na^+ channels in stellate cells could exhibit high levels of persistent activity with little or no transient activity for prolonged periods of time.

Figure 5*A* shows consecutive sweeps at −20 mV from a different experiment that illustrates the properties of a single Na^+ channel exhibiting persistent behavior. This patch contained two channels and displayed both transient and persistent openings in most sweeps. It is most probable that the persistent activity in this patch was mediated by only one of the two channels. The alternative possibility is that the two channels in the patch were independently switching between transient and persistent gating during the experiment, and thus a different channel was mediating persistent openings from one sweep to the next. However, this explanation is unlikely, because we never observed sweeps consisting of overlapping persistent openings, as would be likely to occur if both channels had by chance simultaneously switched to persistent gating. Figure 5*B* shows a diary plot of P_o per sweep for the persistent channel over the course of the 12-min-long experiment. The values were determined from 5 to 500 msec after the start of the test pulse to exclude the transient channel activity, which was clustered near the beginning of each depolarization. P_o values were between 0.1 and 0.9 in most sweeps, reflecting the robust persistent activity in this patch throughout the entire experiment. Persistent openings (defined as openings of at least 25 msec in duration) were observed in 54 of 100 test pulses. In a second patch with only one persistent channel, persistent openings were seen in 48 of 80 sweeps. These experiments demonstrate that single Na^+ channels could exhibit high levels of persistent gating behavior for prolonged periods of time. P_o at −20 mV was 0.170 for the channel shown in Figure 5 and 0.176 ± 0.139 for all four persistent oligochannel patches.

The average slope conductance of persistent Na^+ currents in oligochannel patches was 20.7 ± 1.1 pS ($n = 4$) (Fig. 5*C*). These data were pooled with the conductance for sustained currents in macropatches to give a mean slope conductance for persistent Na^+ channels of 19.7 ± 2.1 pS ($n = 12$). This conductance value is statistically significantly higher than the mean conductance of 15.6 pS for fast Na^+ channels in EC neurons ($p < 0.0005$) and higher than values typically reported for neuronal Na^+ channels

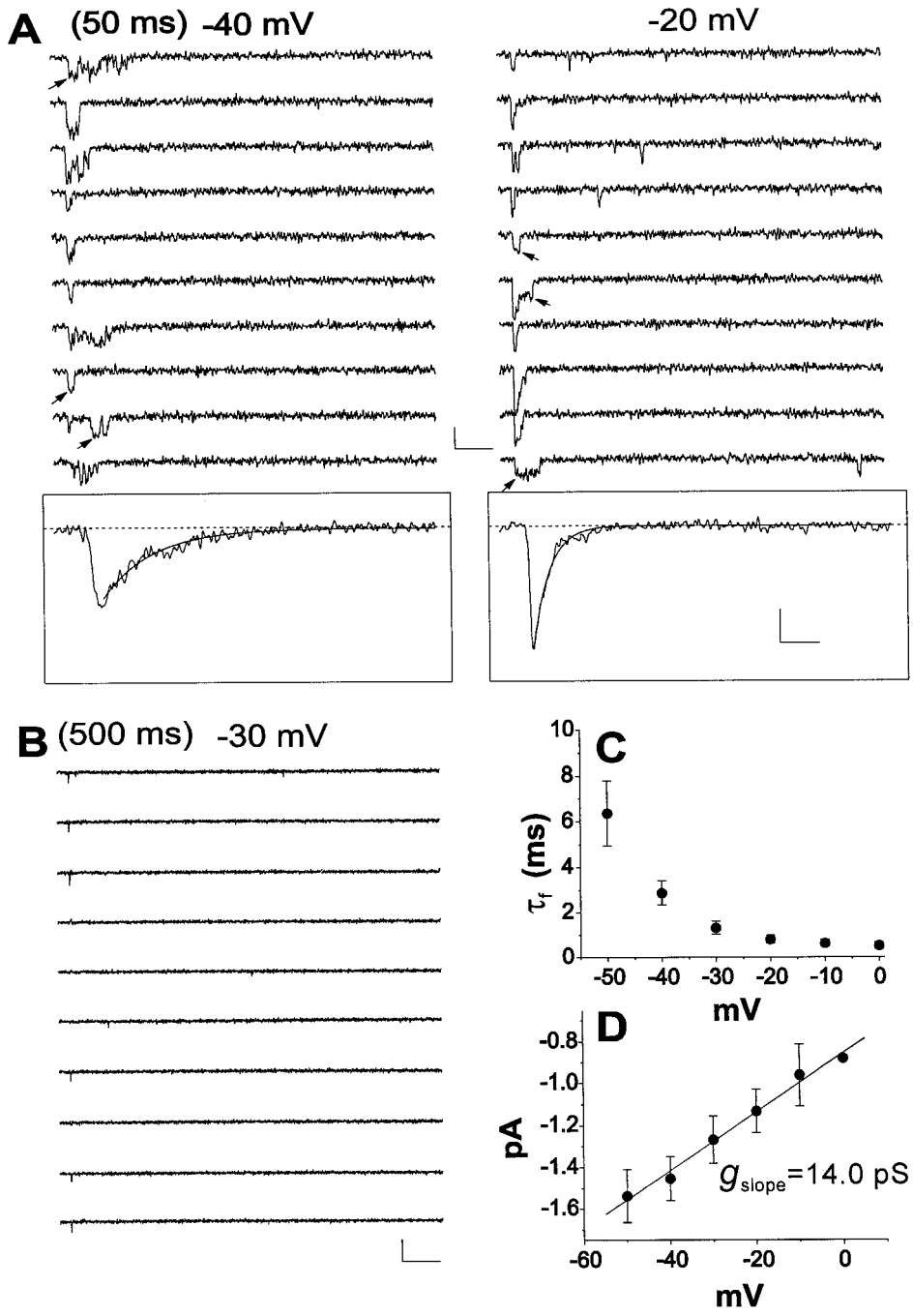

Figure 3. Single-channel currents in oligochannel patches showing exclusively transient activity. *A*, Na^+ channel currents evoked by 50 msec depolarizing pulses to −40 or −20 mV in a patch containing at least three transient Na^+ channels. Calibration: 2 pA, 5 msec. *Insets* show ensemble currents from 20 consecutive traces, along with single exponential fits of the current decay. Time constants were 2.55 (−40 mV) and 0.84 (−20 mV) msec. Calibration: *inset*, 0.5 pA, 2 msec. *B*, Current traces elicited by consecutive 500 msec depolarizing pulses to −30 mV in the same patch as in *A*. Calibration: 2 pA, 50 msec. *C*, Mean values for inactivation time constants, determined by exponential fits of ensemble currents from eight patches containing only transient Na^+ channels. The data were plotted as a function of test potential. *D*, Voltage dependence of transient single-channel current amplitude. To ensure that conductance measurements were not distorted by brief openings that are truncated because of the low-pass filter, only unequivocal, square single-channel openings, such as those indicated by *arrows* in *A*, were considered for these measurements. Data points are from seven patches.

in other single-channel studies (Kirsch and Brown, 1989; Alzheimer et al., 1993; Magee and Johnston, 1995).

DISCUSSION

The entorhinal cortex, hippocampal formation, and perirhinal cortex form a medial temporal lobe memory system that is critical for early stages of declarative memory formation (Scoville and Milner, 1957; Squire and Zola, 1996). The entorhinal cortex has a key location within this circuitry (Suzuki and Amaral, 1994). Multimodal sensory information from various regions of neocortex converge on EC layers II and III, which then convey this information to the dentate gyrus of the hippocampal formation by way of the perforant path. Hippocampal outputs, primarily from CA1 and subiculum, project to EC layers V–VI, which in turn send outputs that reciprocate the neocortical inputs to the entorhinal cortex. In addition, EC layers V–VI project to superficial EC layers, closing an EC–hippocampal loop. Layer II stellate cells, the focus of this study, are a major group of glutamatergic projection neurons that contribute to the perforant path connecting entorhinal cortex to the hippocampus. A striking intrinsic property of stellate cells is that they are capable of generating sustained 5–10 Hz subthreshold oscillations in membrane potential (Alonso and Llinás, 1989). These subthreshold oscillations are proposed to play a role in the genesis of the temporal lobe theta rhythm, which is thought to be important for binding of polymodal information from different cortical regions (Winson,

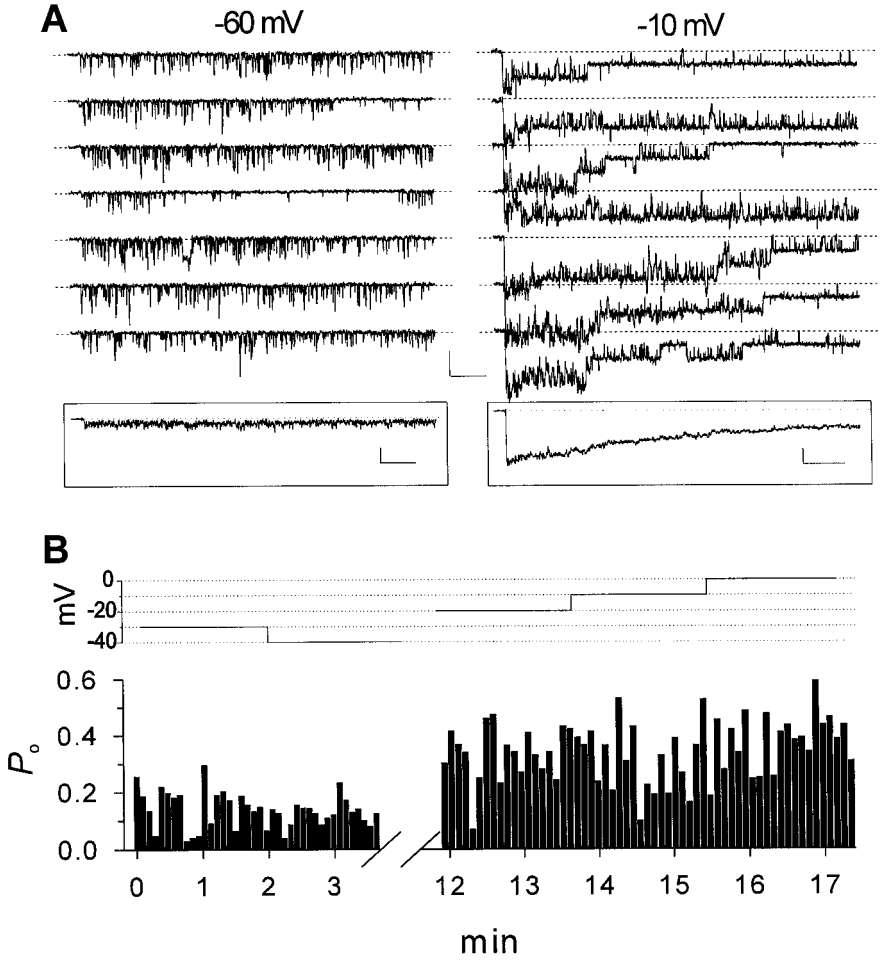

Figure 4. Single-channel currents in a patch exhibiting a high level of persistent activity. *A*, Na^+ channel currents evoked by consecutive 500 msec depolarizing pulses to −60 or −10 mV. Calibration: 2 pA, 50 msec. *Insets* show ensemble average currents obtained from sets of 20 consecutive sweeps. Calibration: *right inset*, 0.5 pA, 50 msec; *left inset*, 1 pA, 50 msec. *B*, Plot of P_o for individual 500-msec-long test pulses in the same experiment as in *A*. Each *bar* corresponds to a single sweep. The test-potential levels are depicted in the *top*. The omitted time interval corresponds to recordings at more negative test potentials (−50 to −80 mV).

1978; Holscher et al., 1997). Furthermore, the intrinsic oscillatory behavior of entorhinal cortex neurons, combined with the reverberatory and highly plastic nature of the EC–hippocampal circuitry may contribute to epileptogenesis in the temporal lobe (Dickson and Alonso, 1997; Klink and Alonso, 1997). Previous work has shown that I_{NaP} contributes to the depolarizing phase of stellate cell oscillations, whereas the repolarizing phase of the oscillations is attributable to the deactivation of a hyperpolarization-activated cation current (I_h) (Alonso and Llinás, 1989; Dickson and Alonso, 1998).

Our results show that I_{NaP} in EC stellate cells is caused by Na^+ channel behavior that is distinguished from conventional transient Na^+ channel activity responsible for I_{Na} by a sustained, high open probability throughout long depolarizations, as well as a significantly higher single-channel conductance. In patches containing persistent channel activity, prolonged late openings were seen in the majority of sweeps throughout experiments lasting up to 17 min. In macropatch recordings, which give an approximation of the channels in the whole-cell soma, persistent Na^+ channel openings represented a small fraction of the total Na^+ channel activity. However, this persistent channel activity contributed a persistent component to ensemble currents that was comparable with whole-cell I_{NaP} in both voltage dependence of activation (10 mV more negative than the transient current) and amplitude (~1% of the transient current at −20 mV). The observation that averaged macropatch recordings can accurately reproduce both the transient and persistent components of whole-cell Na^+ currents supports the hypothesis that the persistent Na^+ channel activity detected in these patches is responsible for whole-cell I_{NaP} in stellate cells. This persistent channel behavior is responsible for the emergence of a cellular property, theta subthreshold oscillations, which is implicated in governing the population behavior of the entorhinal–hippocampal network.

Biophysical mechanisms for I_{NaP} in brain neurons

A number of hypotheses have been proposed to explain persistent Na^+ currents. For example, it has been suggested that I_{NaP} results from a window current attributable to the overlap between channel steady-state activation and inactivation (Attwell et al., 1979) or from slow closed-state inactivation at intermediate membrane potentials (Cummins et al., 1998). One widely held hypothesis is that I_{NaP} results from transitions of conventional transient Na^+ channels to noninactivating gating modes. Slow-mode gating of Na^+ channels was first observed in heart (Patlak and Ortiz, 1985) and skeletal muscle (Patlak and Ortiz, 1986) and in *Xenopus* oocytes expressing cloned Na^+ channel α subunits (Moorman et al., 1990; Zhou et al., 1991). Subsequently, several studies have demonstrated that transient Na^+ channels in brain neurons can also switch to slow gating modes (Alzheimer et al., 1993; Segal and Douglas, 1997). However, in these studies, transitions to slow gating behavior were extremely rare and short-lived events. For example, in multichannel patches from neocortex neurons, bursts of persistent activity were observed in only 1% of test depolarizations (Alzheimer et al., 1993). Compared with this type of

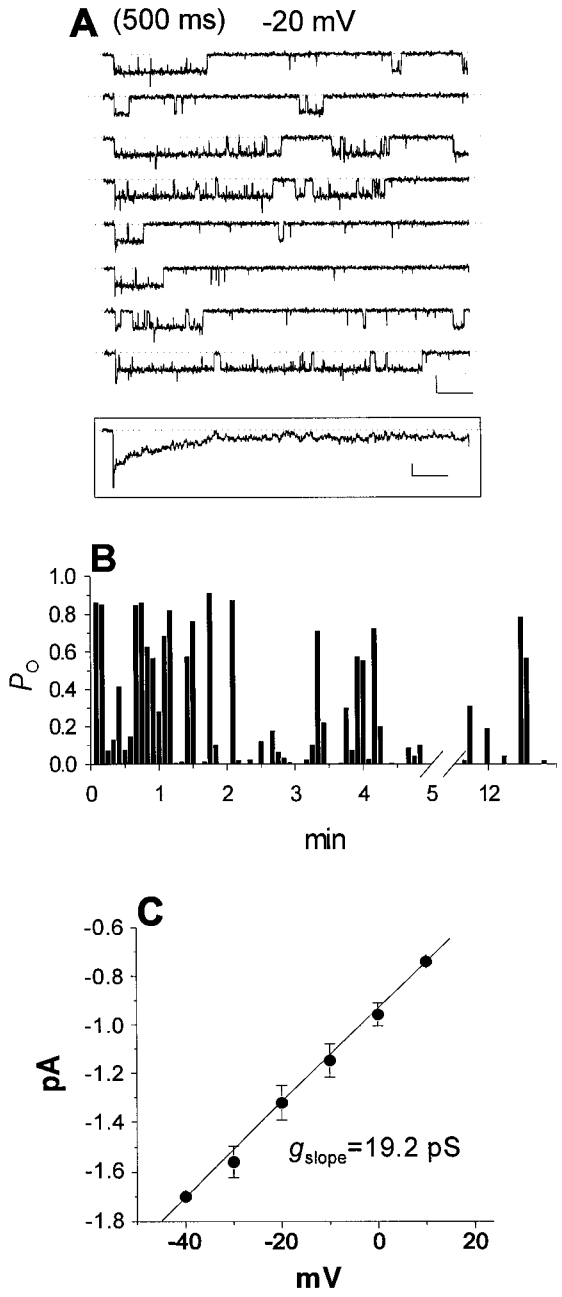

Figure 5. Single-channel currents in a patch containing both a persistent Na^+ channel and a transient Na^+ channel. *A*, Consecutive sweeps recorded in response to 500 msec depolarizing pulses to -20 mV. Calibration: 1 pA, 50 msec. *Inset*, Ensemble current obtained from a set of 20 consecutive traces. Calibration: *inset*, 0.2 pA, 50 msec. *B*, P_o values per sweep for the experiment shown in *A*. *C*, Mean voltage dependence of persistent single-channel current amplitude determined from four persistent Na^+ channel patches.

channel behavior, the persistent activity that we observed in stellate cells was much more stable. For example, in the two patches containing only a single persistent Na^+ channel, we observed prolonged openings in >50% of test depolarizations. Furthermore, the persistent channel activity in stellate cells had a higher single-channel conductance than the transient channel activity, whereas previously described persistent gating modes had the same conductance as transient openings (Alzheimer et al., 1993). Other single-channel studies have suggested that a similar type of stable persistent Na^+ channel activity may be responsible for I_{NaP} in cultured hippocampal neurons (Masukawa et al., 1991) and cerebellar Purkinje cells (Sugimori et al., 1994), although in Purkinje cells, the reported single-channel conductance was only 7 pS. Thus, stable persistent Na^+ channel activity may be a widespread mechanism for generating I_{NaP} in brain neurons. The results presented here add to these previous single-channel studies in several ways. First, we describe persistent activity that is stable throughout long experiments. Second, we demonstrate that this persistent activity has a higher single-channel conductance than transient activity. Third, we show that persistent activity can sum to give the low-threshold persistent Na^+ current seen in whole-cell recordings.

Intracellular application of proteolytic enzymes can destroy sodium channel inactivation (Armstrong et al., 1973). Thus, it may be argued that the persistent channel activity described in this study resulted from the proteolytic treatment used to dissociate EC neurons. However, several observations argue against this explanation. First, in whole-cell recordings of stellate cells in slices, we observed persistent sodium currents with the same relative amplitude and the same biophysical properties as the whole-cell persistent sodium currents in dissociated stellate cells (Magistretti and Alonso, 1999). This finding indicates that persistent sodium currents in dissociated cells are not a consequence of the dissociation procedure. Second, persistent single-channel activity in stellate cells exhibited a single-channel conductance that was significantly higher than the conductance of the transient activity. In contrast, moderate intracellular proteolytic treatment does not typically result in changes in single-channel conductance (Cukierman, 1991; Valenzuela and Bennett, 1994).

Molecular basis for persistent Na^+ channel activity

Although we do not know the molecular basis for persistent Na^+ channel activity in EC stellate cells, we can envision a number of plausible hypotheses. At one extreme, transient and persistent activity could be caused by distinct Na^+ channel isoforms. Alternatively, the same channels could mediate both transient and persistent activity, perhaps with channel kinetics and conductance regulated by phosphorylation, auxiliary subunits, or some other type of long-lasting modulation. In between these two extremes is the possibility that some types of transient Na^+ channels may be particularly predisposed to modulation to persistent gating modes, whereas others are more dedicated to transient gating.

Brain Na^+ channels consist of a pore-forming α subunit that associates with two smaller auxiliary subunits, designated $\beta1$ and $\beta2$ (for review, see Ragsdale and Avoli, 1998). The α subunit is the main molecular determinant of Na^+ channel behavior. Brain neurons express multiple α subunit isoforms, encoded by at least four genes, designated Scn1a, Scn2a, Scn3a, and Scn8a. Preliminary results using reverse transcription-PCR suggest that α subunits encoded by all four of these genes are expressed in cells from adult rat entorhinal cortex (L. Meadows, J. Magistretti, A. Alonso, and D. S. Ragsdale, unpublished observations). Thus, α subunits encoded by one of these genes could mediate persistent channel activity (Joho et al., 1990; Raman et al., 1997; Smith and Goldin, 1998; Smith et al., 1998). Alternatively, persistent activity could be mediated by a novel α subunit isoform that has yet to be cloned and/or yet to be functionally characterized. Other possible explanations for persistent activity include modulation of channel function by β subunits (Isom et al., 1992), phosphorylation (Numann et al., 1991), or direct G-protein interactions (Ma et al., 1997). Ultimately, the molecular basis for persistent Na^+ currents

will most likely be determined using expression of cloned Na^+ channel subunits in heterologous cell systems. The findings presented in this study provide new functional data in brain neurons against which these subsequent molecular analyses will need to be compared and evaluated.

REFERENCES

Aldrich RW, Corey DP, Stevens CF (1983) A reinterpretation of mammalian sodium channel gating based on single channel recording. Nature 306:436–441.

Alonso A, García-Austt E (1987) Neuronal sources of theta rhythm in the entorhinal cortex of the rat. II. Phase relations between unit discharges and theta field potentials. Exp Brain Res 67:502–509.

Alonso A, Llinás RR (1989) Subthreshold Na^+-dependent theta-like rhythmicity in stellate cells of entorhinal cortex layer II. Nature 342:175–177.

Alzheimer C, Schwindt PC, Crill WE (1993) Modal gating of Na^+ channels as a mechanism of persistent Na^+ current in pyramidal neurons from rat and cat sensorimotor cortex. J Neurosci 13:660–673.

Armstrong CM, Bezanilla F, Rojas E (1973) Destruction of sodium conductance inactivation in squid axons perfused with pronase. J Gen Physiol 62:375–391.

Attwell D, Cohen I, Eisner D, Ohba M, Ojeda C (1979) The steady state TTX-sensitive ("window") sodium current in cardiac Purkinje fibres. Pflügers Arch 379:137–142.

Bland BH (1986) The physiology and pharmacology of hippocampal formation theta rhythms. Prog Neurobiol 26:1–54.

Crill WE (1996) Persistent sodium current in mammalian central neurons. Annu Rev Physiol 58:349–362.

Cukierman S (1991) Inactivation modifiers of Na^+ currents and the gating of rat brain Na^+ channels in planar lipid membranes. Pflügers Arch 419:514–521.

Cummins TR, Howe JR, Waxman SG (1998) Slow closed-state inactivation: a novel mechanism underlying ramp currents in cells expressing the hNE/PN1 sodium channel. J Neurosci 18:9607–9619.

Dickson CT, Alonso A (1997) Muscarinic induction of synchronous population activity in the entorhinal cortex. J Neurosci 17:6729–6744.

Dickson CT, Alonso A (1998) Role of I_h in the generation of subthreshold membrane potential oscillations (MPOs) of entorhinal cortex (EC) layer II stellate cells. Soc Neurosci Abstr 24:2035.

Franceschetti S, Guatteo E, Panzica F, Sancini G, Wanke E, Avanzini G (1995) Ionic mechanisms underlying burst firing in pyramidal neurons: intracellular study in rat sensorimotor cortex. Brain Res 696:127–139.

French CR, Sah P, Buckett KS, Gage PW (1990) A voltage-dependent persistent sodium current in mammalian hippocampal neurons. J Gen Physiol 95:1139–1157.

Hamill OP, Marty A, Neher E, Sakmann B, Sigworth FJ (1981) Improved patch clamp techniques for high-resolution current recording from cells and cell-free membrane patches. Pflügers Arch 391:85–100.

Holscher C, Anwyl R, Rowan MJ (1997) Stimulation on the positive phase of hippocampal theta rhythm induces long-term potentiation that can be depotentiated by stimulation on the negative phase in area CA1 *in vivo*. J Neurosci 17:6470–6477.

Isom LL, De Jong KS, Patton DE, Reber BFX, Offord J, Charbonneau T, Scheuer T, Catterall WA (1992) Primary structure and functional expression of the β1 subunit of the rat brain sodium channel. Science 256:839–842.

Joho RH, Moorman JR, VanDongen AM, Kirsch GE, Silberberg H, Schuster G, Brown AM (1990) Toxin and kinetic profile of rat brain type III sodium channels expressed in *Xenopus* oocytes. Mol Brain Res 7:105–113.

Kirsch GE, Brown AM (1989) Kinetic properties of single sodium channels in rat heart and rat brain. J Gen Physiol 93:85–99.

Klink R, Alonso A (1993) Ionic mechanisms for the subthreshold oscillations and differential electroresponsiveness of medial entorhinal cortex layer II neurons. J Neurophysiol 70:144–157.

Klink R, Alonso A (1997) Muscarinic modulation of the oscillatory and repetitive firing properties of entorhinal cortex layer II neurons. J Neurophysiol 77:1813–1828.

Llinás RR, Sugimori M (1980) Electrophysiological properties of in vitro Purkinje cell somata in mammalian cerebellar slices. J Physiol (Lond) 305:197–213.

Ma JY, Catterall WA, Scheuer T (1997) Persistent sodium currents through brain sodium channels induced by G-protein $\beta\gamma$ subunits. Neuron 19:443–452.

Magee JC, Johnston D (1995) Characterization of single voltage-gated Na^+ and Ca^{2+} channels in apical dendrites of rat CA1 pyramidal neurons. J Physiol (Lond) 487:67–90.

Magistretti J, Alonso A (1999) Slow voltage-dependent inactivation of a sustained sodium current in stellate cells of rat entorhinal cortex layer II. In: Molecular and functional diversity of ion channels and receptors (Rudy B, Seeburg P, eds). Ann NY Acad Sci 868:84–88.

Magistretti J, de Curtis M (1998) Low-voltage activated T-type calcium currents are differently expressed in superficial and deep layers of guinea pig piriform cortex. J Neurophysiol 79:808–816.

Masukawa LM, Hansen AJ, Sheperd G (1991) Distribution of single-channel conductances in cultured rat hippocampal neurons. Cell Mol Neurobiol 11:231–243.

Moorman JR, Kirsch GE, VanDongen AMJ, Joho RH, Brown AM (1990) Fast and slow gating of sodium channels encoded by a single mRNA. Neuron 4:243–252.

Numann R, Catterall WA, Scheuer T (1991) Functional modulation of brain sodium channels by protein kinase C phosphorylation. Science 254:115–118.

Parri HR, Crunelli V (1998) Sodium current in rat and cat thalamocortical neurons: role of a non-inactivating component in tonic and burst firing. J Neurosci 18:854–867.

Patlak JB, Ortiz M (1985) Slow currents through single sodium channels of the adult rat heart. J Gen Physiol 86:89–104.

Patlak JB, Ortiz M (1986) Two modes of gating during late Na^+ channel currents in frog sartorius muscle. J Gen Physiol 87:305–326.

Ragsdale DS, Avoli M (1998) Sodium channels as molecular targets for antiepileptic drugs. Brain Res Rev 26:16–28.

Raman IM, Sprunger LK, Meisler MH, Bean BP (1997) Altered subthreshold sodium currents and disrupted firing patterns in Purkinje neurons of Scn8a mutant mice. Neuron 19:881–891.

Scoville WB, Milner B (1957) Loss of recent memory after bilateral hippocampal lesions. J Neurol Neurosurg Psychiatry 20:11–21.

Segal MM (1994) Endogenous bursts underlie seizurelike activity in solitary excitatory hippocampal neurons in microcultures. J Neurophysiol 72:1874–1884.

Segal MM, Douglas AF (1997) Late sodium channel openings underlying epileptiform activity are preferentially diminished by the anticonvulsant phenytoin. J Neurophysiol 77:3021–3034.

Silva LR, Amitai, Y, Connors, BW (1991) Intrinsic oscillations of neocortex generated by layer 5 pyramidal neurons. Science 251:432–434.

Smith MR, Smith RD, Plummer NW, Meisler MH, Goldin AL (1998) Functional analysis of the mouse Scn8a sodium channel. J Neurosci 18:6093–6102.

Smith RD, Goldin AL (1998) Functional analysis of the rat I sodium channel in *Xenopus* oocytes. J Neurosci 18:811–820.

Squire LR, Zola SM (1996) Structure and function of declarative and nondeclarative memory systems. Proc Natl Acad Sci USA 93:13515–13522.

Stuart G, Sakmann B (1995) Amplification of EPSPs by axosomatic sodium channels in neocortical pyramidal neurons. Neuron 15:1065–1076.

Stys PK, Sontheimer H, Ransom BR, Waxman SG (1993) Noninactivating, tetrodotoxin-sensitive Na^+ conductance in rat optic nerve axons. Proc Natl Acad Sci USA 90:6976–6980.

Sugimori M, Kay AR, Llinás R (1994) The persistent Na^+ channel in cerebellar Purkinje cells has a single channel conductance distinct from the inactivating current. Soc Neurosci Abstr 20:63.

Suzuki W, Amaral DG (1994) Topographic organization of the reciprocal connections between the monkey entorhinal cortex and the perirhinal and parahippocampal cortices. J Neurosci 14:1856–1877.

Taylor CP (1993) Na^+ channels that fail to inactivate. Trends Neurosci 16:455–460.

Valenzuela C, Bennett Jr PB (1994) Gating of cardiac Na^+ channels in excised membrane patches after modification by α-chymotrypsin. Biophys J 67:161–171.

Winson J (1978) Loss of hippocampal theta rhythm results in spatial memory deficit in the rat. Science 201:160–163.

Zhou JY, Potts JF, Trimmer JS, Agnew WS, Sigworth FJ (1991) Multiple gating modes and the effect of modulating factors on the mircoI sodium channel. Neuron 7:775–785.